

Article

Bis-Cyclometalated Indazole and Benzimidazole Chiral-at-Iridium Complexes: Synthesis and Asymmetric Catalysis

Sebastian Brunen, Yvonne Grell, Philipp S. Steinlandt, Klaus Harms  and Eric Meggers * 

Fachbereich Chemie, Philipps-Universität Marburg, Hans-Meerwein-Strasse 4, 35043 Marburg, Germany; sbrunen@kofo.mpg.de (S.B.); Grell@staff.uni-marburg.de (Y.G.); philipp.steinlandt@googlemail.com (P.S.S.); xray15@posteo.de (K.H.)

* Correspondence: meggers@chemie.uni-marburg.de

Abstract: A new class of bis-cyclometalated iridium(III) catalysts containing two inert cyclometalated 6-*tert*-butyl-2-phenyl-2*H*-indazole bidentate ligands or two inert cyclometalated 5-*tert*-butyl-1-methyl-2-phenylbenzimidazoles is introduced. The coordination sphere is complemented by two labile acetonitriles, and a hexafluorophosphate ion serves as a counterion for the monocationic complexes. Single enantiomers of the chiral-at-iridium complexes (>99% *er*) are obtained through a chiral-auxiliary-mediated approach using a monofluorinated salicyloxazoline and are investigated as catalysts in the enantioselective conjugate addition of indole to an α,β -unsaturated 2-acyl imidazole and an asymmetric Nazarov cyclization.

Keywords: cyclometalation; chiral-at-metal; asymmetric catalysis



Citation: Brunen, S.; Grell, Y.; Steinlandt, P.S.; Harms, K.; Meggers, E. Bis-Cyclometalated Indazole and Benzimidazole Chiral-at-Iridium Complexes: Synthesis and Asymmetric Catalysis. *Molecules* **2021**, *26*, 1822. <https://doi.org/10.3390/molecules26071822>

Academic Editor: Vincent Ritleng

Received: 12 March 2021

Accepted: 22 March 2021

Published: 24 March 2021

Publisher's Note: MDPI stays neutral with regard to jurisdictional claims in published maps and institutional affiliations.



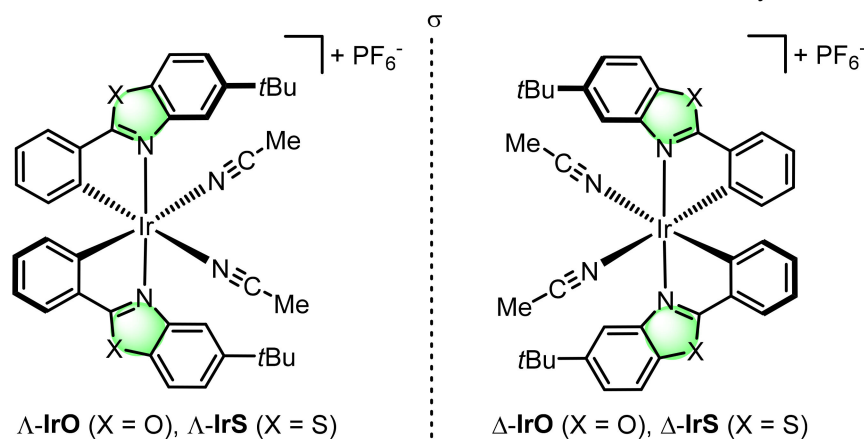
Copyright: © 2021 by the authors. Licensee MDPI, Basel, Switzerland. This article is an open access article distributed under the terms and conditions of the Creative Commons Attribution (CC BY) license (<https://creativecommons.org/licenses/by/4.0/>).

1. Introduction

Cyclometalated transition metal complexes are not only of tremendous importance as intermediates in C–H functionalization reactions but have also gained increasing attention for their interesting catalytic and biological properties, not least due to the pioneering contributions of the Pfeffer laboratory on the formation and applications of metallacycles [1–4]. Our group has recently introduced bis-cyclometalated iridium and rhodium complexes as chiral catalysts for application in asymmetric catalysis [5,6]. Our initial design was based on iridium(III) complexes in which two inert cyclometalated 5-*tert*-butyl-2-phenylbenzoxazoles (**IrO** [7]) or 5-*tert*-butyl-2-phenylbenzothiazoles (**IrS** [8]) are complemented by two labile acetonitrile molecules and hexafluorophosphate served as the counterion for the monocationic complexes (Figure 1a). The two cyclometalated ligands implement a stereogenic metal center with either a left-handed (Λ -configuration) or right-handed (Δ -configuration) overall helical topology [9–21]. The strongly σ -donating phenyl ligands labilize the acetonitrile ligands by exerting a strong *trans* effect [22]. This is important for catalysis, during which one or two acetonitrile ligands are replaced by a substrate or reagent, while the helically arranged inert cyclometalated ligands provide the asymmetric induction.

Since the nature of the cyclometalating ligands affects the reactivity and stereoselectivity of the cyclometalated complexes during catalysis, as has been already witnessed in the differences between benzoxazole and benzothiazole catalysts [5], we aimed to investigate related complexes in which the benzoxazole or benzothiazole heterocycles were replaced with different heterocyclic ligands [23]. Here, we report our results on two new classes of bis-cyclometalated chiral-at-iridium catalysts, which are based on cyclometalated 6-*tert*-butyl-2-phenyl-2*H*-indazoles (Λ - and Δ -**IrInd**) or 5-*tert*-butyl-1-methyl-2-phenylbenzimidazoles (Λ - and Δ -**IrBim**) (Figure 1b). We disclose the synthesis of enantiomerically pure complexes and provide initial results of catalytic asymmetric transformations.

a) Previous Work: Chiral-at-iridium benzoxazole and benzothiazole catalysts



b) This Work: Chiral-at-iridium indazole and benzimidazole catalysts

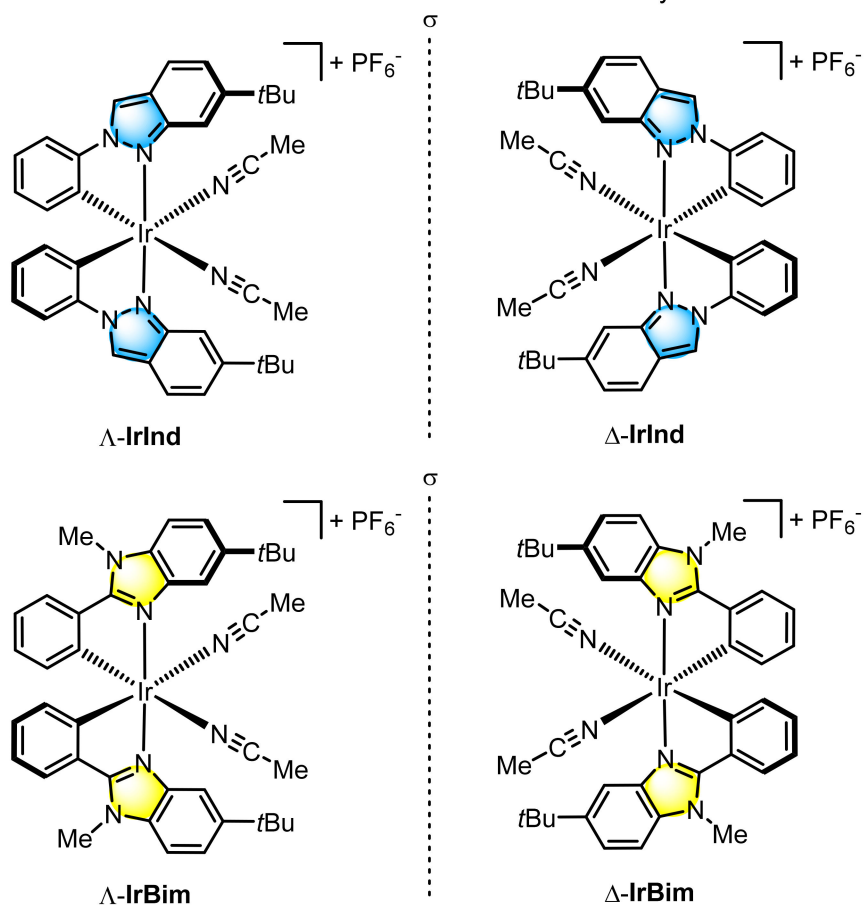


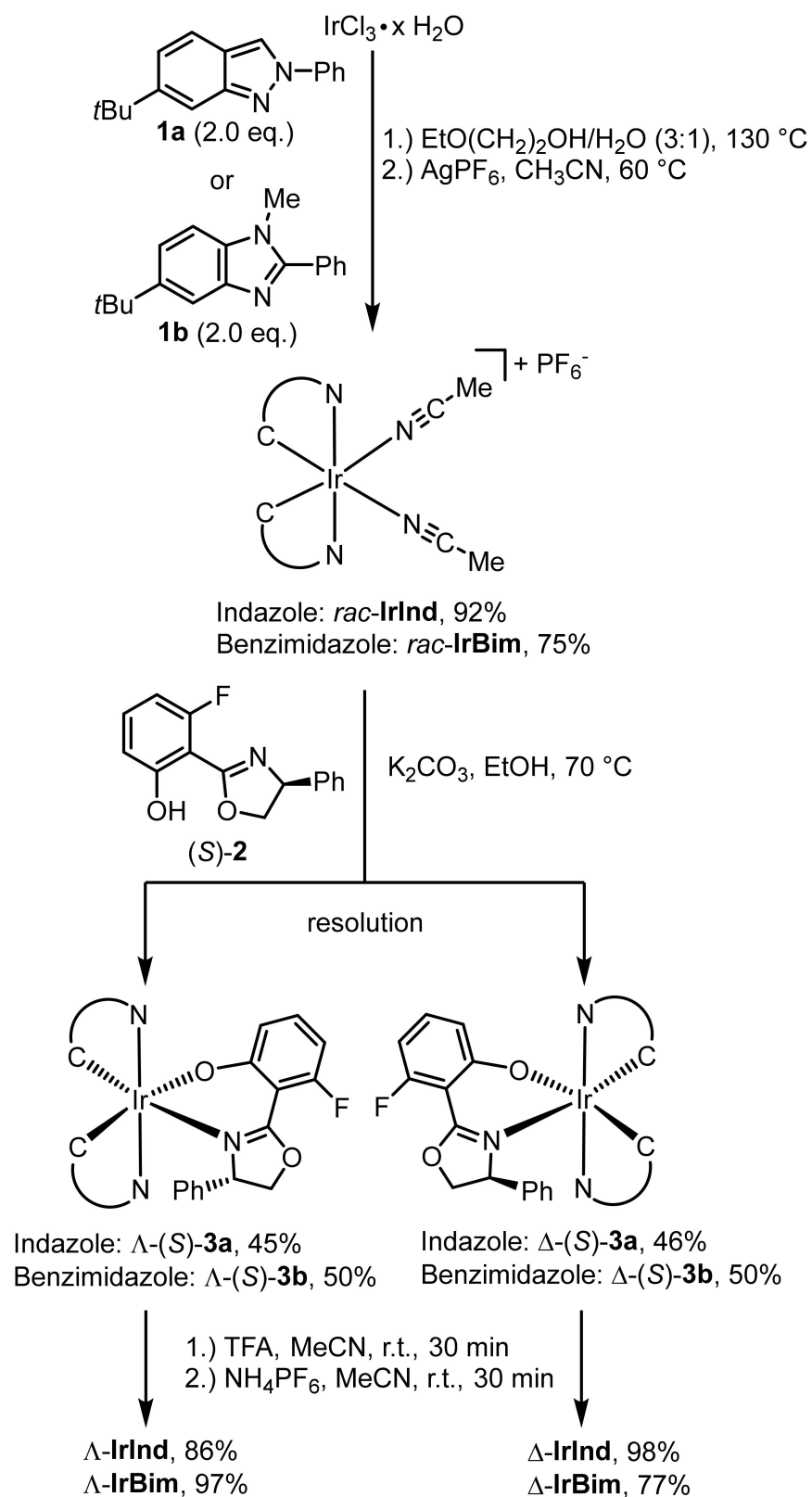
Figure 1. Bis-cyclometalated chiral-at-iridium catalysts for asymmetric conversions. (a) Our most successful previous design. (b) This study.

2. Results and Discussion

Racemic bis-cyclometalated iridium complexes with cyclometalated 2-phenyl-2*H*-indazole [24–27] or 2-phenylbenzimidazole [28–32] ligands are well established but the catalytic properties of non-racemic complexes have not yet been reported. The chiral-auxiliary-mediated [33–36] synthesis of enantiomerically pure complexes **IrInd** and **IrBim**

was performed in analogy to **IrO** [7] and **IrS** [8] and started with the reaction of iridium chloride hydrate with two equivalents of 6-*tert*-butyl-2-phenyl-2*H*-indazole (**1a**) or 5-*tert*-butyl-1-methyl-2-phenylbenzimidazole (**1b**) in a mixture of 2-ethoxyethanol and water (3:1) at 130 °C for 24 h, followed by treatment with silver hexafluorophosphate in acetonitrile to afford *rac*-**IrInd** in 92% yield and *rac*-**IrBim** in 75% yield (Scheme 1). The smooth bis-cyclometalation to provide *rac*-**IrInd** was noteworthy and the yield was significantly higher compared to *rac*-**IrBim** and the previously reported *rac*-**IrO** and *rac*-**IrS** [7,8]. It is interesting to note that the related rhodium benzimidazole complex could not be obtained by this route and stopped after the first cyclometalation step [37,38]. Next, for obtaining single enantiomers, the racemic iridium complexes were reacted with the monofluorinated salicyloxazoline (**S**-2 [39,40] in EtOH at 70 °C for 6 hours in the presence of 3.0 equivalents of K₂CO₃. This converted the racemic mixtures into pairs of diastereomers, which could easily be separated by standard silica gel chromatography (see Figure 2a for an example). For the indazole ligand, Λ -(**S**)-**3a** was obtained in 45% yield and Δ -(**S**)-**3a** in 46% yield, while for the benzimidazole ligand, Λ -(**S**)-**3b** and Δ -(**S**)-**3b** were both obtained in 50% yield. The relative and absolute configuration of Λ -(**S**)-**3b** was determined by single-crystal X-ray diffraction (Figure 2b), and the other complexes were assigned accordingly with the help of circular dichroism (see Supporting Information). The diastereomeric purity of the complexes was investigated by NMR spectroscopy. Figure 2c shows the ¹⁹F-NMR spectra of Λ -(**S**)-**3b** and Δ -(**S**)-**3b**, which demonstrate the high diastereomeric purities of the isolated auxiliary-coordinated complexes. Such high diastereomeric purities are crucial for later obtaining enantiomerically pure catalysts. Finally, cleavage of the auxiliary was conducted with trifluoroacetic acid (TFA) (6.0 equivalents) in MeCN for 30 min at room temperature, and subsequent treatment with NH₄PF₆ provided the individual non-racemic complexes Λ -**IrInd** (86%), Δ -**IrInd** (98%), Λ -**IrBim** (97%), and Δ -**IrBim** (77%) as hexafluorophosphate salts. HPLC analysis on a chiral stationary phase revealed that all four complexes were virtually enantiomerically pure, with enantiomeric ratios of larger than 99:1 (see Supporting Information for HPLC traces). The CD spectra in Figure 3 for Λ - and Δ -**IrInd** demonstrate the mirror-image character of the isolated complexes. The assigned absolute configurations were also confirmed with a crystal structure of Λ -**IrInd** (Figure 4).

Next, we investigated the catalytic properties of the new chiral-at-iridium complexes. Over the past several years, we [5] and others [41–43] have demonstrated that bis-cyclometalated iridium(III) complexes are versatile chiral Lewis acid catalysts. To compare the catalytic activity of the new indazole complex **IrInd** and the benzimidazole complex **IrBim** with the established benzoxazole catalyst **IrO** [7] and benzothiazole catalyst **IrS** [8,44], we chose the enantioselective Friedel–Crafts alkylation of indole with the α,β -unsaturated 2-acyl imidazole **4** (Table 1) [45–48]. At a catalyst loading of 2.0 mol%, Λ -**IrInd** afforded (**S**)-**5** in 84% yield and with 98.5% ee, while Δ -**IrBim** (2.0 mol%) provided (**R**)-**5** in a lower yield of 81% and with slightly decreased 98% ee. In this reaction, **IrBim** also showed lower catalytic activity and required a reaction time of 49 hours, compared to 29 hours for **IrInd**, to complete the reaction at room temperature. However, both catalysts displayed markedly lower catalytic activities compared to the benzoxazole **IrO** and the benzothiazole **IrS**, which could be used at the reduced catalyst loading of just 1.0 mol%. Furthermore, Λ -**IrS** provided (**S**)-**5** with a superior enantiomeric excess of 99% ee [44].



Scheme 1. Auxiliary-mediated synthesis of enantiopure Δ - and Δ -**IrInd**, and Δ - and Δ -**IrBim**.

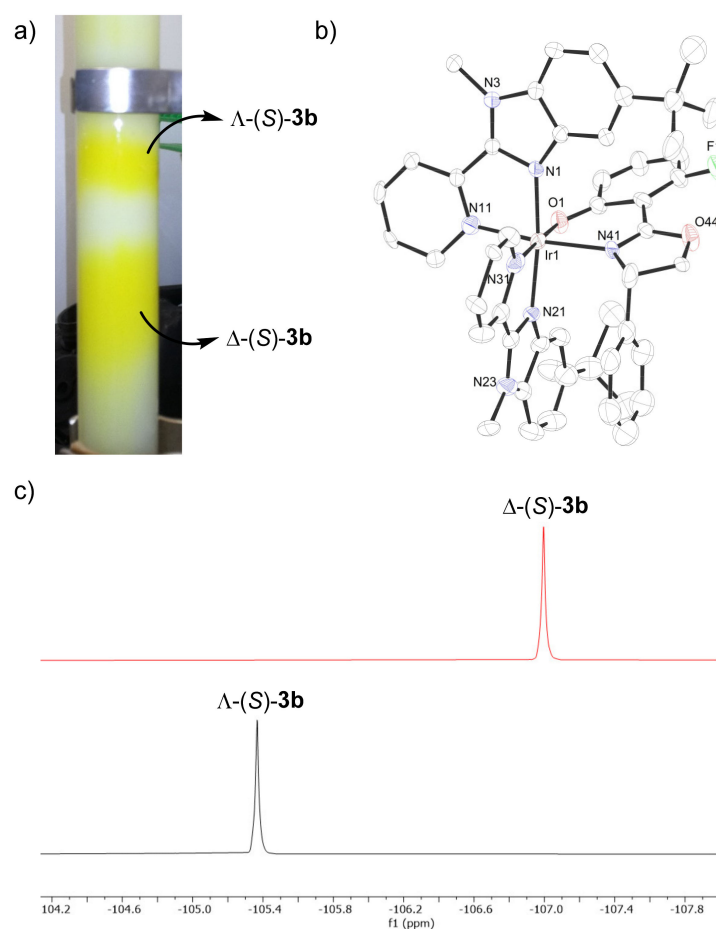


Figure 2. Auxiliary complexes of the iridium benzimidazole system. **a)** Chromatographic separation of Λ -(S)-3b and Δ -(S)-3b during silica gel column chromatography (*n*-pentane/EtOAc). **b)** Single-crystal X-ray structure of Λ -(S)-3b. ORTEP drawing with 30% probability thermal ellipsoids. Solvent molecules are omitted for clarity. **c)** ^{19}F -NMR spectra of the individual diastereomers Λ -(S)-3b and Δ -(S)-3b.

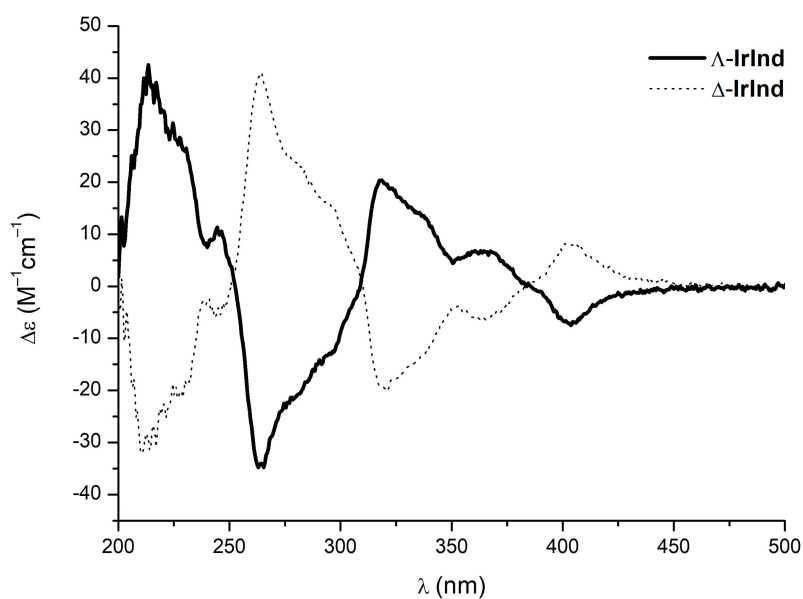


Figure 3. CD spectra of Λ - and Δ -IrInd in MeOH (0.2 mM).

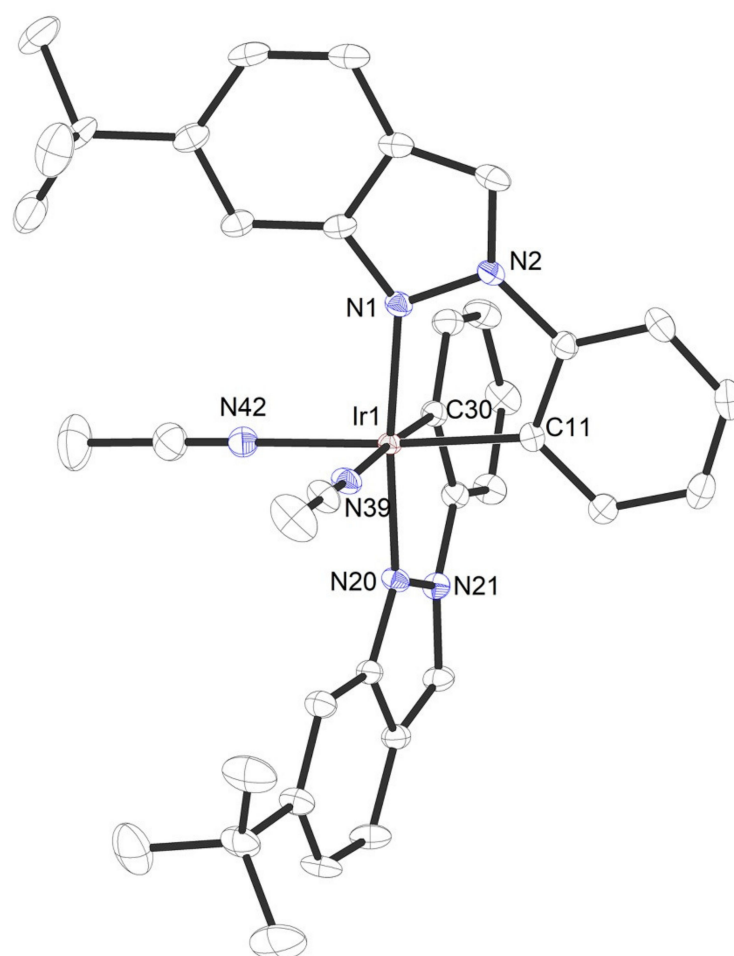


Figure 4. Crystal structure of Δ -IrInd. ORTEP drawing with 30% probability thermal ellipsoids. Hexafluorophosphate counterion and solvent molecules are omitted for clarity.

Table 1. Catalytic enantioselective conjugate addition of indole to 2-acyl imidazole **4**^a.

Entry	Catalyst	Loading (mol%)	Time (h)	Yield ^b	ee ^c
1	Δ -IrInd	2.0	29	84 (S)	98.5
2	Δ -IrBim	2.0	49	81 (R)	98
3 ^d	Δ -IrO	1.0	20	97 (S)	96
4 ^e	Δ -IrS	1.0	40	94 (S)	99

^a Reaction conditions: 2-Acyl imidazole **4** (0.30 mmol), indole (0.75 mmol), and iridium catalyst (1.0 or 2.0 mol%) in THF (0.3 mL) stirred under nitrogen at room temperature for the indicated time. ^b Isolated yields of (S)- or (R)-**5**. ^c Determined by HPLC on a chiral stationary phase. ^d Taken from ref. [4]. ^e Taken from ref. [44].

As a second model reaction, we chose an asymmetric Nazarov cyclization [49,50]. We recently demonstrated that Δ -IrS (2.0 mol%) is an excellent chiral Lewis acid for the conversion of ketoester **6** to the cyclopentenone (1*R*,2*S*)-**7** (Table 2) [51]. Using the same established reaction conditions, after a reaction time of 7 hours in hexafluoroisopropanol [52] at 50 °C, followed by base-induced isomerization to the thermodynamic *trans* diastereomer, (1*R*,2*S*)-**7** was obtained in 75% yield with 15:1 dr and 93% ee. For comparison, IrInd and

IrBim displayed somewhat lower catalytic activity and required an elongated reaction time of 24 hours but, at the same time, afforded higher enantioselectivities compared to **IrS**. Accordingly, Λ -**IrInd** (2.0 mol%) provided (1*R*,2*S*)-**7** in a moderate 46% yield with 11:1 dr and 96% ee, while Δ -**IrBim** (2.0 mol%) provided (1*S*,2*R*)-**7** in 73% yield with 12.5:1 dr and 94% ee.

Table 2. Catalytic asymmetric Nazarov cyclization ^a.

Reaction scheme: Ketoester **6** (with a phenyl group and a methyl ester group) reacts with an iridium catalyst (**Ir-cat**) in hexafluoroisopropanol (**HFIP**) at 50 °C to yield the indole derivative **(1*R*,2*S*)- or (1*S*,2*R*)-7**.

Entry	Catalyst (mol%)	Time (h)	Yield ^b	<i>trans/cis</i>	ee ^c
1 ^d	Λ - IrS (2.0)	7	75% (1 <i>R</i> ,2 <i>S</i>)	15:1	93
2	Λ - IrInd (2.0)	24	46% (1 <i>R</i> ,2 <i>S</i>)	11:1	96
3	Δ - IrBim (2.0)	24	73% (1 <i>S</i> ,2 <i>R</i>)	12.5:1	94

^a Reaction conditions: Ketoester **6** (0.09 mmol) with iridium catalyst (2.0 mol%) in hexafluoroisopropanol (**HFIP**, 0.3 mL), first sonicated and then stirred under a nitrogen atmosphere for the indicated time. Afterwards, the solvent was exchanged for **CH₂Cl₂** and the mixture was stirred in the presence of basic **Al₂O₃** at room temperature for 24 h. ^b Isolated yields of (*S*)- or (*R*)-**5**. ^c Determined by HPLC on a chiral stationary phase. ^d Taken from ref. [51].

3. Materials and Methods

All reactions were carried out under an atmosphere of nitrogen with magnetic stirring in flame-dried glassware, unless stated otherwise. Catalytic reactions were performed in Schlenk tubes (10 mL). Solvents were distilled under nitrogen from sodium/benzophenone (**THF**, **Et₂O**) or calcium hydride (**MeCN**, **CH₂Cl₂**, **CHCl₃**, toluene). Commercially purchased compounds were used without further purification. Flash column chromatography was performed with silica gel 60 M from Macherey-Nagel (irregular shaped, 230–400 mesh, pH 6.8, pore volume: 0.81 mL g⁻¹, mean pore size: 66 Å, specific surface: 492 m² g⁻¹, particle size distribution: 0.5% < 25 µm and 1.7% > 71 µm, water content: 1.6%). ¹H NMR, ¹³C{¹H} NMR, and ¹⁹F{¹H, ¹³C} NMR spectra were recorded on a Bruker AV II 300-MHz, AV III HD 250-MHz, AVIII 500-MHz, AV III HD 500-MHz, or AV II 600-MHz spectrometer at room temperature. The chemical shift δ is listed in ppm with the solvent resonance as internal standard. High-resolution mass spectrometry was conducted via the electrospray ionization technique (**ESI**) or atmospheric pressure chemical ionization technique (**APCI**) on a Finnigan LTQ-FT Ultra mass spectrometer (Thermo Fischer Scientific, Bremen, Germany). CD spectra were recorded on a JASCO J-810 CD spectropolarimeter (parameters: path length of cuvette 1.0 mm, bandwidth 1 nm, data pitch 0.5 nm, response 1 second, sensitivity standard, scanning speed 50 nm/min, accumulation of 3 scans).

rac-IrInd. Iridium(III) chloride hydrate ($w_{\text{Ir}} = 53\%$, 350 mg, 0.97 mmol, 1.00 equiv.) and 6-(*tert*-butyl)-2-phenyl-2*H*-indazole (483 mg, 1.93 mmol, 2.00 equiv.) were added to a Schlenk flask, a mixture of 2-ethoxyethanol and **H₂O** (*v/v* = 3:1, 40 mL, 0.025 M) was added and the resulting suspension was heated to 130 °C for 24 h. The mixture was cooled to room temperature, concentrated under reduced pressure and the obtained residue was dried under vacuum. **AgPF₆** (736 mg, 2.91 mmol, 3.00 equiv.) and **MeCN** (25 mL, 0.04 M) were added, and the resulting suspension was heated to 60 °C for 14 h. The obtained suspension was cooled to room temperature, filtered through a short plug of Celite, rinsed with **MeCN** and concentrated under reduced pressure. The crude product was purified via silica gel column chromatography (**CH₂Cl₂/MeCN** 20:1 → 10:1) to yield **rac-IrInd** (811 mg, 0.88 mmol, 92%) as a yellow solid. TLC: $R_f = 0.48$ (**CH₂Cl₂/MeCN** 10:1). ¹H-NMR: 300 MHz, **CD₂Cl₂**; δ /ppm = 8.68 (s, 2 H, **H_{arom.}**), 7.85 (d, ³*J* = 9.4 Hz, 4 H, **H_{arom.}**), 7.50 (dd,

$^3J = 8.8$ Hz, $^4J = 1.2$ Hz, 2H, $H_{\text{arom.}}$), 7.47 (d, $^3J = 7.9$ Hz, 2H, $H_{\text{arom.}}$), 6.97 (t, $^3J = 7.8$ Hz, 2H, $H_{\text{arom.}}$), 6.64 (t, $^3J = 7.0$ Hz, 2H, $H_{\text{arom.}}$), 5.88 (d, $^3J = 7.3$ Hz, 2H, $H_{\text{arom.}}$), 2.35 (s, 6H, H_{MeCN}), 1.45 (s, 18H, $H_{2\text{xt-butyl}}$). $^{13}\text{C-NMR}$: 75 MHz, CD_2Cl_2 ; $\delta/\text{ppm} = 154.9$ (2C), 148.8 (2C), 143.4 (2C), 134.3 (2C), 127.7 (2C), 127.6 (2C), 124.1 (2C), 124.0 (2C), 122.0 (2C), 121.6 (2C), 120.8 (2C), 120.3 (2C), 113.3 (2C), 109.3 (2C), 36.1 (2C), 31.3 (6C), 4.1 (2C). $^{19}\text{F-NMR}$: 282 MHz, CD_2Cl_2 ; $\delta/\text{ppm} = -72.67$ (d, $J_{\text{P-F}} = 712.6$ Hz, 6F). HRMS: (ESI+, m/z) calc. for $\text{C}_{38}\text{H}_{40}\text{IrN}_6$ [M-PF₆]: 773.2944, found: 773.2940.

rac-IrBim. Iridium(III) chloride hydrate ($w_{\text{Ir}} = 53\%$, 400 mg, 1.10 mmol, 1.00 equiv.) and 5-(*tert*-butyl)-1-methyl-2-phenyl-1*H*-benzo[*d*]imidazole (583 mg, 2.21 mmol, 2.00 equiv.) were added to a Schlenk flask, a mixture of 2-ethoxyethanol and H_2O ($v/v = 3:1$, 44 mL, 0.025 M) was added and the resulting suspension was heated to 130 °C for 24 h. The mixture was cooled to room temperature, concentrated under reduced pressure and the obtained residue was dried under vacuum. AgPF_6 (832 mg, 3.30 mmol, 3.00 equiv.) and MeCN (27 mL, 0.04 M) were added and the resulting suspension was heated to 60 °C for 14 h. The obtained suspension was cooled to room temperature, filtered through a short plug of Celite, rinsed with MeCN and concentrated under reduced pressure. The crude product was purified via silica gel column chromatography ($\text{CH}_2\text{Cl}_2/\text{MeCN}$ 20:1 \rightarrow 10:1) to yield **rac-IrBim** (776 mg, 0.82 mmol, 75%) as yellow solid. TLC: $R_f = 0.43$ ($\text{CH}_2\text{Cl}_2/\text{MeCN}$ 10:1). $^1\text{H-NMR}$: 300 MHz, CD_2Cl_2 ; $\delta/\text{ppm} = 7.93$ (d, $^4J = 1.3$ Hz, 2H, $H_{\text{arom.}}$), 7.76 (dd, $^3J = 8.0$ Hz, $^4J = 0.7$ Hz, 2H, $H_{\text{arom.}}$), 7.65 (dd, $^3J = 8.8$ Hz, $^4J = 1.7$ Hz, 2H, $H_{\text{arom.}}$), 7.58 (d, $^3J = 8.7$ Hz, 2H, $H_{\text{arom.}}$), 6.96 (dt, $^3J = 7.5$ Hz, $^4J = 1.1$ Hz, 2H, $H_{\text{arom.}}$), 6.69 (dt, $^3J = 7.5$ Hz, $^4J = 1.1$ Hz, 2H, $H_{\text{arom.}}$), 6.19 (dd, $^3J = 7.8$ Hz, $^4J = 0.7$ Hz, 2H, $H_{\text{arom.}}$), 4.32 (s, 6H, H_{methyl}), 2.34 (s, 6H, H_{MeCN}), 1.46 (s, 18H, $H_{2\text{xt-butyl}}$). $^{13}\text{C-NMR}$: 75 MHz, CD_2Cl_2 ; $\delta/\text{ppm} = 163.1$ (2C), 148.6 (2C), 144.9 (2C), 140.4 (2C), 135.3 (2C), 134.2 (2C), 133.8 (2C), 130.0 (2C), 124.9 (2C), 123.0 (2C), 122.9 (2C), 119.9 (2C), 112.5 (2C), 110.6 (2C), 35.5 (2C), 32.8 (2C), 32.1 (6C), 4.2 (2C). $^{19}\text{F-NMR}$: 282 MHz, CD_2Cl_2 ; $\delta/\text{ppm} = -72.99$ (d, $J_{\text{P-F}} = 710.7$ Hz, 6F). HRMS: (ESI+, m/z) calc. for $\text{C}_{40}\text{H}_{44}\text{IrN}_6$ [M-PF₆]: 801.3257, found: 801.3253.

Λ -(S)-3a and Δ -(S)-3a. **rac-IrInd** (250 mg, 0.27 mmol, 1.00 equiv.), (S)-**2** (77.1 mg, 0.30 mmol, 1.10 equiv.), and K_2CO_3 (0.81 mmol, 112 mg, 3.00 equiv.) were added to a Schlenk tube, the tube was evacuated for 5 min and absolute ethanol (11 mL, 0.025 M) was added. The tube was sealed and heated to 70 °C for 6 h under a nitrogen atmosphere. The mixture was diluted with CH_2Cl_2 (10 mL) and filtered through a short plug of Celite. The filtrate was concentrated under reduced pressure and the crude product was purified by silica gel column chromatography (*n*-pentane/EtOAc 20:1 \rightarrow 2:1) to yield **Λ -(S)-3a** (115 mg, 121 μmol , 45%) and **Δ -(S)-3a** (118 mg, 124 μmol , 46%), both as brown solids.

Analytical data for **Λ -(S)-3a**: TLC: $R_f = 0.77$ (*n*-pentane/EtOAc 2:1). $^1\text{H-NMR}$: 300 MHz, CD_2Cl_2 ; $\delta/\text{ppm} = 8.51$ (s, 1H, $H_{\text{arom.}}$), 8.08 (s, 1H, $H_{\text{arom.}}$), 7.77 (s, 1H, $H_{\text{arom.}}$), 7.67 (d, $^3J = 9.0$ Hz, 1H, $H_{\text{arom.}}$), 7.54 (s, 1H, $H_{\text{arom.}}$), 7.44 (d, $^3J = 9.0$ Hz, 1H, $H_{\text{arom.}}$), 7.36 (d, $^3J = 7.9$ Hz, 1H, $H_{\text{arom.}}$), 7.35 (dd, $^3J = 9.0$ Hz, $^4J = 1.3$ Hz, 1H, $H_{\text{arom.}}$), 7.27 (dd, $^3J = 9.0$ Hz, $^4J = 1.4$ Hz, 1H, $H_{\text{arom.}}$), 7.04 (dd, $^3J = 8.0$ Hz, $^4J = 0.8$ Hz, 1H, $H_{\text{arom.}}$), 6.99–6.91 (m, 1H, $H_{\text{arom.}}$), 6.90–6.83 (m, 2H, $H_{\text{arom.}}$), 6.78 (t, $^3J = 7.4$ Hz, 1H, $H_{\text{arom.}}$), 6.65–6.39 (m, 6H, $H_{\text{arom.}}$), 6.19 (d, $^3J = 7.3$ Hz, 2H, $H_{\text{arom.}}$), 5.95 (ddd, $^3J = 12.9$ Hz, $^3J = 8.0$ Hz, $^4J = 0.9$ Hz, 1H, $H_{\text{arom.}}$), 5.58 (dd, $^3J = 7.6$ Hz, $^4J = 1.0$ Hz, 1H, $H_{\text{arom.}}$), 4.92 (dd, $^3J = 9.5$ Hz, $^4J = 4.4$ Hz, 1H, $H_{\text{aliph.}}$), 4.82 (dd, $^3J = 9.7$ Hz, $^3J = 9.6$ Hz, 1H, $H_{\text{aliph.}}$), 4.01 (dd, $^3J = 8.6$ Hz, $^4J = 4.4$ Hz, 1H, $H_{\text{aliph.}}$), 1.43 (s, 9H, $H_{\text{t-butyl}}$), 1.27 (s, 9H, $H_{\text{t-butyl}}$). $^{13}\text{C-NMR}$: 75 MHz, CD_2Cl_2 ; $\delta/\text{ppm} = 173.8$ (d, $J_{\text{C-F}} = 3.3$ Hz), 165.4, 163.2 (d, $J_{\text{C-F}} = 3.6$ Hz), 162.0, 153.5, 153.0, 149.0, 148.4, 145.3, 144.5, 140.7, 138.6, 135.8, 134.6, 133.1 (d, $J_{\text{C-F}} = 14.5$ Hz), 132.0, 128.1, 127.2, 127.0, 126.7, 125.8, 122.8, 122.7, 122.25, 121.5 (d, $J_{\text{C-F}} = 1.8$ Hz), 121.0 (d, $J_{\text{C-F}} = 2.9$ Hz), 120.8, 120.7, 120.4, 120.4, 120.1, 113.2, 113.0, 110.9, 109.8, 109.1, 101.8, 101.7, 100.0, 99.7, 75.9, 70.5, 35.8 (d, $J_{\text{C-F}} = 22.4$ Hz), 31.4 (6C). $^{19}\text{F-NMR}$: 282 MHz, CD_2Cl_2 ; $\delta/\text{ppm} = -105.40$. HRMS: (ESI+, m/z) calc. for $\text{C}_{49}\text{H}_{46}\text{FIrN}_5\text{O}_2$ [M + H]⁺: 948.3265, found: 948.3263. CD (mdeg, 0.05 M in MeOH), λ in nm: 418 (−5), 322 (20), 300 (−6), 285 (−2), 260 (−18), 251 (−13), 234 (−40).

Analytical data for **Δ -(S)-3a**: TLC: $R_f = 0.68$ (*n*-pentane/EtOAc 2:1). $^1\text{H-NMR}$: 300 MHz, CD_2Cl_2 ; $\delta/\text{ppm} = 8.58$ (s, 1H, $H_{\text{arom.}}$), 8.47 (s, 1H, $H_{\text{arom.}}$), 8.23 (s, 1H, $H_{\text{arom.}}$), 7.80 (s, 1H,

H_{arom.}), 7.77 (d, ³J = 9.0 Hz, 1H, H_{arom.}), 7.62 (d, ³J = 8.9 Hz, 1H, H_{arom.}), 7.40 (dd, ³J = 9.1 Hz, ⁴J = 1.5 Hz, 1H, H_{arom.}), 7.36 (d, ³J = 8.0 Hz, 1H, H_{arom.}), 7.29 (dd, ³J = 8.9 Hz, ⁴J = 1.4 Hz, 1H, H_{arom.}), 7.17 (d, ³J = 8.1 Hz, 1H, H_{arom.}), 6.93–6.75 (m, 7H, H_{arom.}), 6.61–6.53 (m, 2H, H_{arom.}), 6.25 (d, ³J = 8.7 Hz, 1H, H_{arom.}), 6.07 (dt, ³J = 7.5 Hz, ⁴J = 0.9 Hz, 1H, H_{arom.}), 5.98–5.90 (m, 2H, H_{arom.}), 5.59 (dd, ³J = 7.7 Hz, ⁴J = 0.8 Hz, 1H, H_{arom.}), 4.27 (dd, ³J = 10.5 Hz, ³J = 9.8 Hz, 1H, H_{aliph.}), 4.05 (t, ³J = 9.3 Hz, 1H, H_{aliph.}), 3.79 (t, ³J = 10.0 Hz, 1H, H_{aliph.}), 1.39 (s, 9H, H_{t-butyl}), 1.23 (s, 9H, H_{t-butyl}). ¹³C-NMR: 76 MHz, CD₂Cl₂; δ/ppm = 174.4 (d, J_{C-F} = 3.6 Hz), 174.3, 164.1 (d, J_{C-F} = 1.5 Hz), 161.5, 153.6, 152.7, 148.9 (d, J_{C-F} = 19.4 Hz), 144.3, 144.0, 140.1, 137.0, 136.8, 134.8, 133.1, 132.9, 132.4, 128.5, 127.8, 127.4, 127.0, 126.6, 123.4, 122.9, 122.3, 121.2, 121.1, 120.9, 120.5, 120.5, 120.2, 120.0 (d, J_{C-F} = 2.6 Hz), 119.9, 112.9, 112.6, 110.5, 103.7 (d, J_{C-F} = 8.2 Hz), 99.8, 99.5, 75.9, 71.1, 36.0, 35.8, 31.4 (d, J_{C-F} = 0.8 Hz), 31.2 (6C). ¹⁹F-NMR: 282 MHz, CD₂Cl₂; δ/ppm = -106.95. HRMS: (ESI+, *m/z*) calc. for C₄₉H₄₆FIrN₅O₂ [M + H]⁺: 948.3265, found: 948.3263. CD (mdeg, 0.05 M in MeOH), λ in nm: 417 (12), 324 (-25), 303 (23), 285 (10), 257 (21), 250 (20), 234 (73).

Λ-(S)-3b and Δ-(S)-3b.rac-IrBim (46 mg, 48.6 μmol, 1.00 equiv.), (S)-2 (13.7 mg, 53.5 μmol, 1.10 equiv.) and K₂CO₃ (20.7 mg, 0.15 mmol, 3.00 equiv.) were added to a Schlenk tube, the tube was evacuated for 5 min and absolute ethanol (2 mL, 0.025 M) was added. The tube was sealed, heated to 70 °C for 6 h under a nitrogen atmosphere and then diluted with CH₂Cl₂ (5 mL) and finally filtered through a short plug of Celite. The filtrate was concentrated under reduced pressure and the crude product was purified by silica gel column chromatography (*n*-pentane/EtOAc 6:1 → 1:1) to yield Λ-(S)-3b (23.9 mg, 24.5 μmol, 50%) and Δ-(S)-3b (24.0 mg, 24.6 μmol, 50%), both as brown solids.

Analytical data for Λ-(S)-3b: TLC: R_f = 0.39 (*n*-pentane/EtOAc 2:1). ¹H-NMR: 300 MHz, CD₂Cl₂; δ/ppm = 8.15 (d, ⁴J = 1.4 Hz, 1H, H_{arom.}), 7.71 (d, ³J = 7.8 Hz, 1H, H_{arom.}), 7.61 (d, ⁴J = 1.2 Hz, 1H, H_{arom.}), 7.49 (dd, ³J = 8.7 Hz, ⁴J = 1.7 Hz, 1H, H_{arom.}), 7.42 (d, ³J = 8.6 Hz, 1H, H_{arom.}), 7.41 (d, ³J = 8.5 Hz, 1H, H_{arom.}), 7.34 (d, ³J = 7.9 Hz, 1H, H_{arom.}), 7.14 (d, ³J = 8.6 Hz, 1H, H_{arom.}), 7.03–6.79 (m, 5H, H_{arom.}), 6.63–6.45 (m, 5H, H_{arom.}), 6.14 (d, ⁴J = 6.9 Hz, 2H, H_{arom.}), 6.03 (dd, ³J = 7.7 Hz, ⁴J = 0.6 Hz, 1H, H_{arom.}), 5.92 (ddd, ³J = 13.0 Hz, ³J = 7.9 Hz, ⁴J = 1.0 Hz, 1H, H_{arom.}), 4.97 (dd, ³J = 9.5 Hz, ⁴J = 4.3 Hz, 1H, H_{aliph.}), 4.82 (t, ³J = 9.2 Hz, 1H, H_{aliph.}), 4.18 (s, 3H, H_{aliph.}), 3.96 (dd, ³J = 8.6 Hz, ⁴J = 4.2 Hz, 1H, H_{aliph.}), 3.78 (s, 3H, H_{aliph.}), 1.44 (s, 9H, H_{t-butyl}), 1.28 (s, 9H, H_{t-butyl}). ¹³C-NMR: 75 MHz, CD₂Cl₂; δ/ppm = 173.7, 165.4, 165.0, 163.2, 162.4, 155.8, 150.0, 147.7, 147.6, 141.8, 141.3, 140.9, 137.2, 136.7, 135.7, 134.2, 133.9, 133.4, 132.7, 132.5, 129.1 (d, J_{C-F} = 3.8 Hz), 127.4, 126.8, 124.9, 124.9, 121.3, 121.3, 121.1, 121.0, 120.2, 114.4, 112.4, 109.8, 109.0, 101.7 (d, J_{C-F} = 6.7 Hz), 99.5, 99.2, 75.6, 75.6, 70.8, 35.5, 35.3, 32.6, 32.2 (3C), 32.2 (3C), 31.8, 30.3. ¹⁹F-NMR: 282 MHz, CD₂Cl₂; δ/ppm = -105.37. HRMS: (ESI+, *m/z*) calc. for C₅₁H₅₀FIrN₅O₂ [M + H]⁺: 976.3578, found: 976.3576. CD (mdeg, 0.05 M in MeOH), λ in nm: 441 (-12), 354 (65), 331 (54), 319 (83), 296 (-46), 292 (-44), 270 (-3), 267 (-5), 252 (29), 224 (-73).

Analytical data for Δ-(S)-3b: TLC: R_f = 0.28 (*n*-pentane/EtOAc 2:1). ¹H-NMR: 300 MHz, CD₂Cl₂; δ/ppm = 8.25 (dd, ⁴J = 1.4 Hz, ⁴J = 0.8 Hz, 1H, H_{arom.}), 7.85 (d, ⁴J = 1.4 Hz, 1H, H_{arom.}), 7.66 (dd, ³J = 7.9 Hz, ⁴J = 0.8 Hz, 1H, H_{arom.}), 7.52–7.46 (m, 3H, H_{arom.}), 7.43 (dd, ³J = 8.7 Hz, ⁴J = 1.7 Hz, 1H, H_{arom.}), 7.34 (d, ³J = 8.7 Hz, 1H, H_{arom.}), 6.93–6.74 (m, 7H, H_{arom.}), 6.60 (dt, ³J = 7.6 Hz, ⁴J = 1.3 Hz, 1H, H_{arom.}), 6.53 (dt, ³J = 7.6 Hz, ⁴J = 1.2 Hz, 1H, H_{arom.}), 6.28 (d, ³J = 8.6 Hz, 1H, H_{arom.}), 6.21 (dd, ³J = 7.6 Hz, ⁴J = 0.8 Hz, 1H, H_{arom.}), 6.07 (dt, ³J = 7.5 Hz, ⁴J = 1.2 Hz, 1H, H_{arom.}), 5.92–5.85 (m, 2H, H_{arom.}), 4.30 (s, 3H, H_{aliph.}), 4.21–4.12 (m, 1H, H_{aliph.}), 4.16 (s, 3H, H_{aliph.}), 4.07–3.99 (m, 2H, H_{aliph.}), 1.38 (s, 9H, H_{t-butyl}), 1.23 (s, 9H, H_{t-butyl}). ¹³C-NMR: 76 MHz, CD₂Cl₂; δ/ppm = 182.0, 179.0, 174.6 (d, mboxemph)J_{C-F} = 3.8 Hz), 165.0, 164.8, 163.1, 163.1, 161.5, 154.1, 151.0, 147.6 (d, J_{C-F} = 86.0 Hz), 141.3 (d, J_{C-F} = 25.3 Hz), 140.7, 136.5, 136.4, 135.3, 134.1, 133.9 (d, J_{C-F} = 20.0 Hz), 132.4 (d, J_{C-F} = 13.6 Hz), 129.0 (d, J_{C-F} = 28.1 Hz), 128.4, 127.6, 127.5, 124.7, 121.5, 121.4, 121.0, 120.2, 120.2, 119.8, 114.1, 113.7, 109.6, 109.5, 103.8, 103.7, 99.2, 98.9, 75.6, 69.9, 35.4, 35.3, 32.4, 32.4, 32.1 (d, J_{C-F} = 0.8 Hz, 3C), 31.9 (3C), 31.2. ¹⁹F-NMR: 282 MHz, CD₂Cl₂; δ/ppm = -107.00. HRMS: (ESI+, *m/z*) calc. for C₅₁H₅₀FIrN₅O₂ [M + H]⁺: 976.3578, found: 976.3576. CD (mdeg, 0.05 M

in MeOH), λ in nm: 444 (23), 321 (−32), 295 (53), 274 (25), 272 (26), 255 (−10), 252 (−11), 224 (78).

Λ - and Δ -IrInd. Λ -(S)-**3a** (97 mg, 0.10 mmol, 1.00 equiv.) or Δ -(S)-**3a** (100 mg, 0.11 mmol, 1.00 equiv) was dissolved in MeCN (5 mL, 0.02 M) and TFA (for Λ -(S)-**3a**: 46 μ L, 0.60 mmol; for Δ -(S)-**3a**: 51 μ L, 0.66 mmol; 6.00 equiv.) was added dropwise. The solution was stirred for 30 min under a nitrogen atmosphere at room temperature and then concentrated under reduced pressure. The residue was redissolved in MeCN (5 mL, 0.02 M), and NH_4PF_6 (for Λ -(S)-**3a**: 326 mg, 2.0 mmol; for Δ -(S)-**3a**: 359 mg, 2.20 mmol; 20.0 equiv.) was added in one portion. The suspension was stirred at room temperature for 30 min, concentrated and purified via silica gel column chromatography ($\text{CH}_2\text{Cl}_2/\text{MeCN}$ 20:1 \rightarrow 10:1) to yield Λ -IrInd (80.7 mg, 88.0 μ mol, 86%) or Δ -IrInd (94.6 mg, 103 μ mol, 98%) as a yellow, crystalline solid.

Analytical data for Λ -IrInd: HPLC: er > 99% (Daicel Chiralpak IB N-5 column, $250 \times 4.6 \text{ m}^2$, 254 nm, 25 $^\circ\text{C}$, 0.6 mL/min, H_2O (+0.1% TFA)/MeCN 60:40 to 50:50 in 180 min, holding 50% MeCN for 250 min, t_r (major) = 186.1 min, t_r (minor) = 182.1 min). CD (mdeg, 0.05 M in MeOH), λ in nm: 403 (−24), 362 (31), 351 (23), 317 (97), 296 (−54), 293 (−53), 263 (−150), 245 (54), 240 (42), 217 (263). All other analytical data were in agreement with the racemic complex.

Analytical data for Δ -IrInd: HPLC: er > 99% (Daicel Chiralpak IB N-5 column, $250 \times 4.6 \text{ m}^2$, 254 nm, 25 $^\circ\text{C}$, 0.6 mL/min, H_2O (+0.1% TFA)/MeCN 60:40 to 50:50 in 180 min, holding 50% MeCN for 250 min, t_r (major) = 182.1 min, t_r (minor) = 186.1 min). CD (mdeg, 0.05 M in MeOH), λ in nm: 402 (20), 365 (−11), 352 (−5), 317 (−41), 263 (102), 245 (−12), 240 (−3), 213 (−175). All other analytical data were in agreement with the racemic complex.

Λ - and Δ -IrBim. Λ -(S)-**3b** (24.0 mg, 24.6 μ mol, 1.00 equiv.) or Δ -(S)-**3b** (80.0 mg, 82.0 μ mol, 1.00 equiv) was dissolved in MeCN (for Λ -(S)-**3b**: 1.25 mL; for Δ -(S)-**3b**: 4.1 mL, 0.02 M) and TFA (for Λ -(S)-**3b**: 11.5 μ L, 0.15 mmol; for Δ -(S)-**3b**: 38 μ L, 0.49 mmol; 6.00 equiv.) was added dropwise. The solution was stirred for 30 min under a nitrogen atmosphere at room temperature and then concentrated under reduced pressure. The residue was redissolved in MeCN (for Λ -(S)-**3b**: 1.25 mL; for Δ -(S)-**3b**: 4.1 mL, 0.02 M) and NH_4PF_6 (for Λ -(S)-**3b**: 81.5 mg, 0.50 mmol; for Δ -(S)-**3b**: 267 mg, 1.64 mmol; 20.0 equiv.) was added in one portion. The suspension was stirred at room temperature for 30 min, concentrated and purified via silica gel column chromatography ($\text{CH}_2\text{Cl}_2/\text{MeCN}$ 20:1 \rightarrow 10:1) to yield Λ -IrBim (22.5 mg, 23.8 μ mol, 97%) or Δ -IrBim (59.8 mg, 63.2 μ mol, 77%) as yellow, crystalline solid.

Analytical data for Λ -IrBim: HPLC: er > 99% (Daicel Chiralpak IB N-5 column, $250 \times 4.6 \text{ m}^2$, 254 nm, 25 $^\circ\text{C}$, 0.6 mL/min, H_2O (+0.1% TFA)/MeCN 60:40 to 50:50 in 180 min, holding 50% MeCN for 250 min, t_r (major) = 190.2 min, t_r (minor) = 177.0 min). CD (mdeg, 0.05 M in MeOH), λ in nm: 427 (−7), 342 (38), 293 (−30), 279 (−20), 265 (−27), 247 (6), 239 (−5), 229 (9), 220 (−14), 212 (79). All other analytical data were in agreement with the racemic complex.

Analytical data for Δ -IrBim: HPLC: er = >99% (Daicel Chiralpak IB N-5 column, $250 \times 4.6 \text{ mm}$, 254 nm, 25 $^\circ\text{C}$, 0.6 mL/min, H_2O (+0.1% TFA)/MeCN 60:40 to 50:50 in 180 min, holding 50% MeCN for 250 min, t_r (major) = 177.0 min, t_r (minor) = 190.2 min). CD (mdeg, 0.05 M in MeOH), λ in nm: 427 (9), 341 (−52), 292 (45), 278 (29), 267 (39), 248 (−7), 239 (9), 227 (−17), 221 (13), 212 (−109). All other analytical data were in agreement with the racemic complex.

Asymmetric Friedel–Crafts reaction. A Schlenk tube was charged with the iridium catalyst (6.0 μ mol, 2 mol%), followed by THF (0.3 mL, 1.0 M) under a nitrogen atmosphere. The α,β -unsaturated 2-acyl imidazole **4** (45.1 mg, 0.30 mmol, 1.00 eq.) was added to the suspension in one portion, whereupon a black solution formed. The solution was stirred for 20 min at room temperature and subsequently treated with indole (87.8 mg, 0.75 mmol, 2.50 eq.). The resulting solution was stirred at room temperature until complete consumption of α,β -unsaturated 2-acyl imidazole **4** was detected by TLC. The solution was

concentrated under reduced pressure and purified via silica gel column chromatography (*n*-pentane/EtOAc 1.5:1 to 1:1) to yield the Friedel–Crafts adduct (*S*)- or (*R*)-**5** as a white solid. The enantiomeric excess was determined by chiral HPLC analysis (Daicel Chiralpak IC column, 250 × 4.6 m², absorbance at 254 nm, column temperature 40 °C, mobile phase *n*-hexane/*i*-PrOH 90:10, flow rate 0.5 mL/min, *t_r* (major) = 23.7 min, *t_r* (minor) = 28.3 min).

Asymmetric Nazarov cyclization. A Schlenk tube was charged with the iridium catalyst (1.8 μmol, 2 mol%), an *E/Z* mixture of indole-functionalized α -unsaturated β -ketoester **6** (27.5 mg, 0.09 mmol, 1.00 eq.) and HFIP (0.3 mL, 0.3 M) under a nitrogen atmosphere. The mixture was homogenized via sonication (1 min) and subsequently placed in a preheated oil bath at 50 °C. The solution was stirred at 50 °C until the complete consumption of used α -unsaturated β -ketoester **6** was indicated via TLC analysis. The solvent was then removed under reduced pressure and the diastereomeric ratio was determined via ¹H-NMR analysis. The crude product was redissolved in CH₂Cl₂, transferred into a 10 mL-flask and basic Al₂O₃ (Sigma Aldrich, Darmstadt, Germany, 58 Å pore size, pH 9.5 ± 0.5 in water, 140 mg) was added in one portion. The suspension was stirred for 24 h and filtered over a cotton plug subsequently. The obtained solution was concentrated under reduced pressure and purified via silica gel column chromatography (*n*-pentane/EtOAc 3:1 to 2:1) to give the desired cyclized product **7**. The Al₂O₃-equilibrated diastereomeric ratio was determined via ¹H-NMR analysis and the enantiomeric excess for the major diastereomer (*trans*-diastereomer **7**) was determined via chiral HPLC analysis (Daicel Chiralpak AD-H column, 250 × 4.6 m², absorbance at 254 nm, column temperature 25 °C, mobile phase *n*-hexane/*i*-PrOH 90:10, flow rate 0.6 mL/min, *t_r* (major) = 21.0 min, *t_r* (minor) = 30.3 min).

Single-crystal X-ray diffraction. Crystal structure data can be accessed via the Cambridge Crystallographic Data Centre (CCDC) under the deposition numbers 2069740 (Λ -**IrInd**), 2069741 (*rac*-**IrBim**), and 2069742 (Λ -(*S*)-**3b**).

4. Conclusions

In conclusion, we introduced two new bis-cyclometalated iridium(III) catalysts containing two inert cyclometalated 6-*tert*-butyl-2-phenyl-2*H*-indazole bidentate ligands or two inert cyclometalated 5-*tert*-butyl-1-methyl-2-phenylbenzimidazoles, together with two labile acetonitriles and a hexafluorophosphate counterion. These complexes complement previously reported related benzoxazole and benzothiazole complexes and thereby expand the family of bis-cyclometalated chiral-at-iridium catalysts for application in asymmetric catalysis. The reasons for the differences in the catalytic activity and stereoselectivity of the catalysts after replacing benzoxazole or benzothiazole with indazole or benzimidazole moieties need to be examined. Future work will also investigate their properties as catalysts for asymmetric photochemistry.

Supplementary Materials: The following are available online, NMR spectra, HPLC traces, and crystallographic data.

Author Contributions: Conceptualization, E.M.; methodology, S.B., Y.G., P.S.S. and K.H.; validation, S.B., Y.G., P.S.S. and K.H.; formal analysis, S.B., Y.G., P.S.S. and K.H.; investigation, S.B., Y.G., P.S.S.; resources, E.M. and K.H.; data curation, S.B., Y.G., P.S.S. and K.H.; writing—original draft preparation, E.M.; writing—review and editing, S.B., Y.G. and P.S.S.; supervision, E.M.; project administration, E.M.; funding acquisition, E.M. All authors have read and agreed to the published version of the manuscript.

Funding: This research was funded by the Deutsche Forschungsgemeinschaft (ME1805/17-1).

Data Availability Statement: All data are contained within the article and the Supplementary Materials.

Conflicts of Interest: The authors declare no conflict of interest. The funders had no role in the design of the study; in the collection, analyses, or interpretation of data; in the writing of the manuscript, or in the decision to publish the results.

Sample Availability: Samples of the compounds are not available from the authors.

References

1. Ritleng, V.; Sirlin, C.; Pfeffer, M. Ru-, Rh-, and Pd-Catalyzed C–C Bond Formation Involving C–H Activation and Addition on Unsaturated Substrates: Reactions and Mechanistic Aspects. *Chem. Rev.* **2002**, *102*, 1731–1770. [[CrossRef](#)]
2. Albrecht, M. Cyclometalation Using d-Block Transition Metals: Fundamental Aspects and Recent Trends. *Chem. Rev.* **2010**, *110*, 576–623. [[CrossRef](#)] [[PubMed](#)]
3. Djukic, J.-P.; Sortais, J.-B.; Barloy, L.; Pfeffer, M. Cycloruthenated Compounds—Synthesis and Applications. *Eur. J. Inorg. Chem.* **2009**, 817–853. [[CrossRef](#)]
4. Gaiddon, C.; Pfeffer, M. The Fate of Cycloruthenated Compounds: From C-H Activation to Innovative Anticancer Therapy. *Eur. J. Inorg. Chem.* **2017**, 1639–1654. [[CrossRef](#)]
5. Zhang, L.; Meggers, E. Steering Asymmetric Lewis Acid Catalysis Exclusively with Octahedral Metal-Centered Chirality. *Acc. Chem. Res.* **2017**, *50*, 320–330. [[CrossRef](#)] [[PubMed](#)]
6. Huang, X.; Meggers, E. Asymmetric Photocatalysis with Bis-cyclometalated Rhodium Complexes. *Acc. Chem. Res.* **2019**, *52*, 833–847. [[CrossRef](#)] [[PubMed](#)]
7. Huo, H.; Fu, C.; Harms, K.; Meggers, E. Asymmetric Catalysis with Substitutionally Labile yet Stereochemically Stable Chiral-at-Metal Iridium(III) Complex. *J. Am. Chem. Soc.* **2014**, *136*, 2990–2993. [[CrossRef](#)] [[PubMed](#)]
8. Huo, H.; Shen, X.; Wang, C.; Zhang, L.; Röse, P.; Chen, L.-A.; Harms, K.; Marsch, M.; Hilt, G.; Meggers, E. Asymmetric photoredox transition-metal catalysis activated by visible light. *Nature* **2014**, *515*, 100–103. [[CrossRef](#)]
9. Pierre, J.-L. Enantioselective creation of helical chirality in octahedral (OC-6) complexes. Recent advances. *Coord. Chem. Rev.* **1998**, *178–180*, 1183–1192. [[CrossRef](#)]
10. Brunner, H. Optically Active Organometallic Compounds of Transition Elements with Chiral Metal Atoms. *Angew. Chem. Int. Ed.* **1999**, *38*, 1194–1208. [[CrossRef](#)]
11. Knof, U.; Von Zelewsky, A. Predetermined Chirality at Metal Centers. *Angew. Chem. Int. Ed.* **1999**, *38*, 302–322. [[CrossRef](#)]
12. Knight, P.D.; Scott, P. Predetermination of chirality at octahedral centres with tetradentate ligands: Prospects for enantioselective catalysis. *Coord. Chem. Rev.* **2003**, *242*, 125–143. [[CrossRef](#)]
13. Ganter, C. Chiral organometallic half-sandwich complexes with defined metal configuration. *Chem. Soc. Rev.* **2003**, *32*, 130–138. [[CrossRef](#)] [[PubMed](#)]
14. Fontecave, M.; Hamelin, O.; Ménage, S. Chiral-at-Metal Complexes in Asymmetric Catalysis. *Top. Organomet. Chem.* **2005**, *15*, 271–288.
15. Meggers, E. Asymmetric Synthesis of Octahedral Coordination Complexes. *Eur. J. Inorg. Chem.* **2011**, 2911–2926. [[CrossRef](#)]
16. Bauer, E.B. Chiral-at-metal complexes and their catalytic applications in organic synthesis. *Chem. Soc. Rev.* **2012**, *41*, 3153–3167. [[CrossRef](#)]
17. Constable, E.C. Stereogenic metal centres—From Werner to supramolecular chemistry. *Chem. Soc. Rev.* **2013**, *42*, 1637–1651. [[CrossRef](#)] [[PubMed](#)]
18. Von Zelewsky, A. Stereochemistry of Coordination Compounds: From Alfred Werner to the 21st Century. *Chimia* **2014**, *68*, 297–298. [[CrossRef](#)]
19. Gong, L.; Chen, L.-A.; Meggers, E. Asymmetric Catalysis Mediated by the Ligand Sphere of Octahedral Chiral-at-Metal Complexes. *Angew. Chem. Int. Ed.* **2014**, *53*, 10868–10874. [[CrossRef](#)]
20. Zhang, L.; Meggers, E. Stereogenic-Only-at-Metal Asymmetric Catalysts. *Chem. Asian J.* **2017**, *12*, 2335–2342. [[CrossRef](#)] [[PubMed](#)]
21. Cruchter, T.; Larionov, V.A. Asymmetric catalysis with octahedral stereogenic-at-metal complexes featuring chiral ligands. *Coord. Chem. Rev.* **2018**, *376*, 95–113. [[CrossRef](#)]
22. Coe, B.J.; Glenwright, S.J. Trans-effects in octahedral transition metal complexes. *Coord. Chem. Rev.* **2000**, *203*, 5–80. [[CrossRef](#)]
23. See also: Li, Y.; Lei, M.; Yuan, W.; Meggers, E.; Gong, L. An N-heterocyclic carbene iridium catalyst with metal-centered chirality for enantioselective transfer hydrogenation of imines. *Chem. Commun.* **2017**, *53*, 8089–8092.
24. Tamayo, A.B.; Garon, S.; Sajoto, T.; Djurovich, P.I.; Tsyba, I.M.; Bau, R.; Thompson, M.E. Cationic Bis-cyclometalated Iridium(III) Diimine Complexes and Their Use in Efficient Blue, Green, and Red Electroluminescent Devices. *Inorg. Chem.* **2005**, *44*, 8723–8732. [[CrossRef](#)] [[PubMed](#)]
25. Shavaleev, N.M.; Scopelliti, R.; Grätzel, M.; Nazeeruddin, M.K. Phosphorescent cationic iridium(III) complexes with cyclometalating 1H-indazole and 2H-[1,2,3]-triazole ligands. *Inorg. Chim. Acta* **2012**, *388*, 84–87. [[CrossRef](#)]
26. Zhao, K.-Y.; Shan, G.-G.; Fu, Q.; Su, Z.-M. Tuning Emission of AIE-Active Organometallic Ir(III) Complexes by Simple Modulation of Strength of Donor/Acceptor on Ancillary Ligands. *Organometallics* **2016**, *35*, 3996–4001. [[CrossRef](#)]
27. Niu, Z.-G.; Han, H.-B.; Li, M.; Zhao, Z.; Chen, G.-Y.; Zheng, Y.-X.; Li, G.-N.; Zuo, J.-L. Tunable Emission Color of Iridium(III) Complexes with Phenylpyrazole Derivatives as the Main Ligands for Organic Light-Emitting Diodes. *Organometallics* **2018**, *37*, 3154–3164. [[CrossRef](#)]
28. Huang, W.-S.; Lin, J.T.; Chien, C.-H.; Tao, Y.-T.; Sun, S.-S.; Wen, Y.-S. Highly Phosphorescent Bis-Cyclometalated Iridium Complexes Containing Benzoimidazole-Based Ligands. *Chem. Mat.* **2004**, *16*, 2480–2488. [[CrossRef](#)]
29. Velusamy, M.; Thomas, K.R.J.; Chen, C.-H.; Lin, J.T.; Wen, Y.S.; Hsieh, W.-T.; Lai, C.-H.; Chou, P.-T. Synthesis, structure and electroluminescent properties of cyclometalated iridium complexes possessing sterically hindered ligands. *Dalton Trans.* **2007**, 3025–3034. [[CrossRef](#)] [[PubMed](#)]

30. Li, C.; Zhang, G.; Shih, H.-H.; Jiang, X.; Sun, P.; Pan, Y.; Cheng, C.-H. High-efficient phosphorescent iridium(III) complexes with benzimidazole ligand for organic light-emitting diodes: Synthesis, electrochemistry and electroluminescent properties. *J. Organomet. Chem.* **2009**, *694*, 2415–2420. [[CrossRef](#)]
31. Chen, L.; Ding, J.; Cheng, Y.; Xie, Z.; Wang, L.; Jing, X.; Wang, F. Bipolar Heteroleptic Green Iridium Dendrimers Containing Oligocarbazole and Oxadiazole Dendrons for Bright and Efficient Nondoped Electrophosphorescent Devices. *Chem. Asian J.* **2011**, *6*, 1372–1380. [[CrossRef](#)] [[PubMed](#)]
32. Shan, G.-G.; Li, H.-B.; Sun, H.-Z.; Cao, H.-T.; Zhu, D.-X.; Su, Z.-M. Enhancing the luminescence properties and stability of cationic iridium(III) complexes based on phenylbenzoimidazole ligand: A combined experimental and theoretical study. *Dalton Trans.* **2013**, *42*, 11056–11065. [[CrossRef](#)]
33. Meggers, E. Chiral Auxiliaries as Emerging Tools for the Asymmetric Synthesis of Octahedral Metal Complexes. *Chem. Eur. J.* **2010**, *16*, 752–758. [[CrossRef](#)] [[PubMed](#)]
34. Gong, L.; Wenzel, M.; Meggers, E. Chiral-Auxiliary-Mediated Asymmetric Synthesis of Ruthenium Polypyridyl Complexes. *Acc. Chem. Res.* **2013**, *46*, 2635–2644. [[CrossRef](#)] [[PubMed](#)]
35. Chen, L.-A.; Xu, W.; Huang, B.; Ma, J.; Wang, L.; Xi, J.; Harms, K.; Gong, L.; Meggers, E. Asymmetric Catalysis with an Inert Chiral-at-Metal Iridium Complex. *J. Am. Chem. Soc.* **2013**, *135*, 10598–10601. [[CrossRef](#)] [[PubMed](#)]
36. Ma, J.; Zhang, X.; Huang, X.; Luo, S.; Meggers, E. Preparation of chiral-at-metal catalysts and their use in asymmetric photoredox chemistry. *Nat. Protoc.* **2018**, *13*, 605–632. [[CrossRef](#)] [[PubMed](#)]
37. Grell, Y.; Hong, Y.; Huang, X.; Mochizuki, T.; Xie, X.; Harms, K.; Meggers, E. Chiral-at-Rhodium Catalyst Containing Two Different Cyclometalating Ligands. *Organometallics* **2019**, *38*, 3948–3954. [[CrossRef](#)]
38. Steinlandt, P.S.; Zuo, W.; Harms, K.; Meggers, E. Bis-Cyclometalated Indazole Chiral-at-Rhodium Catalyst for Asymmetric Photoredox Cyanoalkylations. *Chem. Eur. J.* **2019**, *25*, 15333–15340. [[CrossRef](#)]
39. Marchi, E.; Sinisi, R.; Bergamini, G.; Tragni, M.; Monari, M.; Bandini, M.; Ceroni, P. Easy Separation of Δ and Λ Isomers of Highly Luminescent [Ir^{III}]-Cyclometalated Complexes Based on Chiral Phenol-Oxazoline Ancillary Ligands. *Chem. Eur. J.* **2012**, *18*, 8765–8773. [[CrossRef](#)]
40. Ma, J.; Shen, X.; Harms, K.; Meggers, E. Expanding the family of bis-cyclometalated chiral-at-metal rhodium(III) catalysts with a benzothiazole derivative. *Dalton Trans.* **2016**, *45*, 8320–8323. [[CrossRef](#)]
41. Xu, G.-Q.; Liang, H.; Fang, J.; Jia, Z.-L.; Chen, J.-Q.; Xu, P.-F. Catalytic Enantioselective α -Fluorination of 2-Acyl Imidazoles via Iridium Complexes. *Chem. Asian J.* **2016**, *11*, 3355–3358. [[CrossRef](#)] [[PubMed](#)]
42. Deng, T.; Thota, G.K.; Li, Y.; Kang, Q. Enantioselective conjugate addition of hydroxylamines to α,β -unsaturated 2-acyl imidazoles catalyzed by a chiral-at-metal Rh(III) complex. *Chem. Front.* **2017**, *4*, 573–577. [[CrossRef](#)]
43. Liang, H.; Xu, G.-Q.; Feng, Z.-T.; Wang, Z.-Y.; Xu, P.-F. Dual Catalytic Switchable Divergent Synthesis: An Asymmetric Visible-Light Photocatalytic Approach to Fluorine-Containing γ -Keto Acid Frameworks. *J. Org. Chem.* **2019**, *84*, 60–72. [[CrossRef](#)] [[PubMed](#)]
44. Shen, X.; Huo, H.; Wang, C.; Zhang, B.; Harms, K.; Meggers, E. Octahedral Chiral-at-Metal Iridium Catalysts: Versatile Chiral Lewis Acids for Asymmetric Conjugate Additions. *Chem. Eur. J.* **2015**, *21*, 9720–9726. [[CrossRef](#)] [[PubMed](#)]
45. Evans, D.A.; Fandrick, K.R.; Song, H.-J. Enantioselective Friedel–Crafts Alkylations of α,β -Unsaturated 2-Acyl Imidazoles Catalyzed by Bis(oxazolonyl)pyridine–Scandium(III) Triflate Complexes. *J. Am. Chem. Soc.* **2005**, *127*, 8942–8943. [[CrossRef](#)] [[PubMed](#)]
46. Evans, D.A.; Fandrick, K.R. Catalytic Enantioselective Pyrrole Alkylations of α,β -Unsaturated 2-Acyl Imidazoles. *Org. Lett.* **2006**, *8*, 2249–2252. [[CrossRef](#)] [[PubMed](#)]
47. Evans, D.A.; Fandrick, K.R.; Song, H.-J.; Scheidt, K.A.; Xu, R. Enantioselective Friedel–Crafts Alkylations Catalyzed by Bis(oxazolonyl)pyridine–Scandium(III) Triflate Complexes. *J. Am. Chem. Soc.* **2007**, *129*, 10029–10041. [[CrossRef](#)] [[PubMed](#)]
48. Boersma, A.J.; Feringa, B.L.; Roelfes, G. Enantioselective Friedel–Crafts Reactions in Water Using a DNA-Based Catalyst. *Angew. Chem. Int. Ed.* **2009**, *48*, 3346–3348. [[CrossRef](#)] [[PubMed](#)]
49. Shimada, N.; Stewart, C.; Tius, M.A. Asymmetric Nazarov Cyclizations. *Tetrahedron* **2011**, *67*, 5851–5870. [[CrossRef](#)] [[PubMed](#)]
50. Raja, S.; Nakajima, M.; Rueping, M. Experimental and Computational Study of the Catalytic Asymmetric 4π -Electrocyclization of N-Heterocycles. *Angew. Chem. Int. Ed.* **2015**, *54*, 2762–2765. [[CrossRef](#)]
51. Mietke, T.; Cruchter, T.; Larionov, V.A.; Faber, T.; Harms, K.; Meggers, E. Asymmetric Nazarov Cyclizations Catalyzed by Chiral-at-Metal Complexes. *Adv. Synth. Catal.* **2018**, *360*, 2093–2100. [[CrossRef](#)]
52. In previous work we found that hexafluoroisopropanol (HFIP) is a very suitable solvent for this reaction. Since it is a weak acid, we speculate that it facilitates the release of the catalyst-bound product and thereby avoids product inhibition. See Ref. [51] for more details.